MAGNETIC QUENCHING OF α AND DIFFUSIVITY TENSORS IN HELICAL TURBULENCE

Axel Brandenburg,[1] Karl-Heinz Rädler,[2] Matthias Rheinhardt,[2] and Kandaswamy Subramanian[3]

ABSTRACT

The effect of a dynamo-generated mean magnetic field of Beltrami type on the mean electromotive force is studied. In the absence of the mean magnetic field the turbulence is assumed to be homogeneous and isotropic, but it becomes inhomogeneous and anisotropic with this field. Using the test-field method the dependence of the α and turbulent diffusivity tensors on the magnetic Reynolds number Re_M is determined for magnetic fields that have reached approximate equipartition with the velocity field. The tensor components are characterized by a pseudoscalar α and a scalar turbulent magnetic diffusivity η_t. Increasing Re_M from 2 to 600 reduces η_t by a factor ≈5, suggesting that the quenching of η_t is, in contrast to the two-dimensional case, only weakly dependent on Re_M. Over the same range of Re_M, however, α is reduced by a factor ≈14, which can be explained by a corresponding increase of a magnetic contribution to the α-effect with opposite sign. Within this framework, the corresponding kinetic contribution to the α-effect turns out to be independent of Re_M for $2 \leq Re_M \leq 600$. The level of fluctuations of α and η_t is only 10% and 20% of the respective kinematic reference values.

Subject headings: MHD — turbulence

1. INTRODUCTION

Magnetic fields in stars and galaxies tend to display large-scale spatial order, and in the case of the Sun also long-term temporal order (the 22 year cycle). The underlying process is generally believed to be a turbulent large-scale or mean-field dynamo—the simplest of which is an α^2 dynamo, which works with helical turbulence and no mean flows. This can be modeled by direct numerical simulations in a periodic box where the flow is driven by helical isotropic forcing. Corresponding simulations by Brandenburg (2001) show that in the nonlinear regime there is a resistively slow saturation phase associated with nearly perfect conservation of magnetic helicity. This slow saturation imposes tight constraints on the quenching of the electromotive force. By comparing with suitable mean field models one can only constrain the quenching of the full electromotive force, but not the individual quenchings of α and η_t, because the saturated mean magnetic field of an α^2 dynamo tends to become force-free, so the mean magnetic field and the mean current density are aligned (Blackman & Brandenburg 2002, hereafter BB02). As a consequence an infinitude of combinations of quenching expressions for α and η_t describe the same saturation behavior.

The saturation of the mean magnetic field is well described by a mutual cancellation of kinetic and magnetic α-effects, where the latter depends on the production rate of mean magnetic helicity. To reproduce the resistively slow saturation, both kinetic α-effect, α_K, and turbulent magnetic diffusivity, η_t, could be assumed completely unquenched. This is however an unrealistic simplification (Kleeorin & Rogachevskii 1999). Some level of quenching of η_t was found to be necessary to reproduce the simulations (BB02).

Since the early work of Vainshtein & Cattaneo (1992), a lot of effort has gone into determining the quenching of α. It is now clear that for mean fields defined as volume averages over a periodic box α is "catastrophically" quenched like Re_M^{-1} with

mean fields of equipartition strength (Cattaneo & Hughes 1996). However, subsequent work showed that this is a particular consequence of the use of full volume averages, in which case the mean current density is zero (BB02).

The quenching of η_t is much less understood. While in the two-dimensional case, η_t is indeed catastrophically quenched (Cattaneo & Vainshtein 1991), in three dimensions the quenching may depend just on $\overline{\boldsymbol{B}}^2$, but not on Re_M. This has already been found from the decay rate of a nonhelical large-scale magnetic field in driven nonhelical turbulence (Yousef et al. 2003). Similar indications come also from fitting mean field models to corresponding simulations (BB02).

Quantifying more precisely the simultaneous quenching of α and η_t is the goal of the present Letter. We admit both α and η_t to be tensors, denoted by α_{ij} and η_{ij}, respectively, and we calculate them using the test-field method (e.g., Brandenburg et al. 2008; Sur et al. 2008). However, unlike earlier kinematic work, we now allow the velocity to be the result of the fully nonlinear hydromagnetic equations, i.e., to be influenced by the resulting mean magnetic field.

2. THE METHOD

Following earlier work by Brandenburg (2001), we consider a compressible isothermal gas with sound speed c_s, but in addition we also solve a set of test-field equations, as was done in Brandenburg et al. (2008) for the kinematic case. The full set of governing equations is then

$$\frac{\partial \boldsymbol{U}}{\partial t} = -\boldsymbol{U} \cdot \boldsymbol{\nabla} \boldsymbol{U} - c_s^2 \boldsymbol{\nabla} \ln \rho + \boldsymbol{f} + \rho^{-1}(\boldsymbol{J} \times \boldsymbol{B} + \boldsymbol{\nabla} \cdot 2\rho\nu\boldsymbol{S}),$$

(1)

$$\frac{\partial \ln \rho}{\partial t} = -\boldsymbol{U} \cdot \boldsymbol{\nabla} \ln \rho - \boldsymbol{\nabla} \cdot \boldsymbol{U},$$

(2)

$$\frac{\partial \boldsymbol{A}}{\partial t} = \boldsymbol{U} \times \boldsymbol{B} - \mu_0 \eta \boldsymbol{J},$$

(3)

[1] NORDITA, Roslagstullsbacken 23, SE-10691 Stockholm, Sweden.
[2] Astrophysical Institute Potsdam, An der Sternwarte 16, D-14482 Potsdam, Germany.
[3] Inter University Centre for Astronomy and Astrophysics, Post Bag 4, Pune University Campus, Ganeshkhind, Pune 411 007, India.
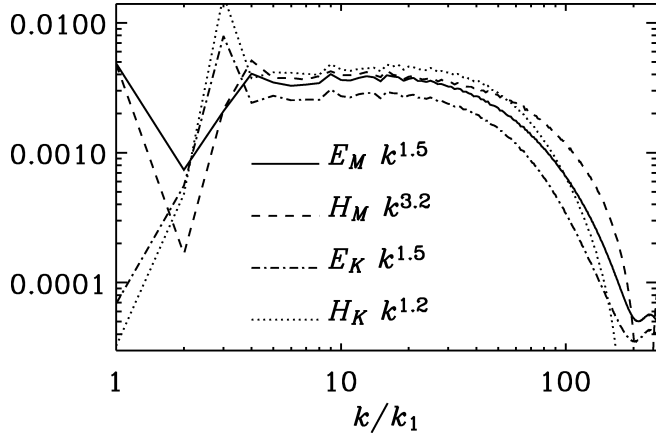
Fig. 1.—Compensated time-averaged spectra of kinetic and magnetic energy, as well as of kinetic and magnetic helicity, for a run with $\mathrm{Re}_M = 600$.

$$\frac{\partial \boldsymbol{a}^{pq}}{\partial t} = \overline{\boldsymbol{U}} \times \boldsymbol{b}^{pq} + \boldsymbol{u} \times \overline{\boldsymbol{B}}^{pq} + \boldsymbol{u} \times \boldsymbol{b}^{pq} - \overline{\boldsymbol{u} \times \boldsymbol{b}^{pq}} - \mu_0 \eta \boldsymbol{j}^{pq},$$

(4)

where mean fields are defined as horizontal (xy) averages, thus being functions of z and t only, and indicated by overbars whereas lowercase vectors denote deviations from the averages ("fluctuations"). The superscripts pq refer to four separate equations that are characterized by four different test fields $\overline{\boldsymbol{B}}^{pq}$ having a $\cos kz$ or $\sin kz$ dependence ($q = $ c, s) in the x or y component ($p = $ 1, 2). We employ a magnetic vector potential both for the magnetic field $\boldsymbol{B} = \nabla \times \boldsymbol{A}$ and for the responses to the test fields, $\boldsymbol{b}^{pq} = \nabla \times \boldsymbol{a}^{pq}$. We reinitialize $\boldsymbol{a}^{pq}$ to zero every 30–60 turnover times to suppress small-scale dynamo action (cf. Sur et al. 2008). Of course, the velocity $\boldsymbol{U}$ is now affected by the magnetic field $\boldsymbol{B}$ through the Lorentz force. The current density is $\boldsymbol{J} = \nabla \times \boldsymbol{B}/\mu_0$, where μ_0 is the magnetic permeability. The flow is driven by random forcing described by a forcing function $\boldsymbol{f}$ consisting of circularly polarized plane waves with positive helicity and random direction (giving rise to a flow with maximal helicity), and $S_{ij} = \frac{1}{2}(U_{i,j} + U_{j,i}) - \frac{1}{3}\delta_{ij}\nabla \cdot \boldsymbol{U}$ is the traceless rate of strain tensor. The forcing function is chosen such that the moduli of the wavevectors, $|\boldsymbol{k}_f|$, are in a narrow interval around an average value, which is denoted simply by k_f.

Owing to our definition of averages, $\overline{\boldsymbol{B}}$ is independent of x and y and all its first-order spatial derivatives can be expressed by the components of $\overline{\boldsymbol{J}}$. If we ignore higher order derivatives of $\overline{\boldsymbol{B}}$ the mean electromotive force $\overline{\mathcal{E}} = \overline{\boldsymbol{u} \times \boldsymbol{b}}$ has the form

$$\overline{\mathcal{E}}_i = \alpha_{ij}\overline{B}_j - \mu_0 \eta_{ij}\overline{J}_j$$

(5)

with two tensors α_{ij} and η_{ij}, and we restrict our attention to $1 \leq i, j \leq 2$. For details see Brandenburg et al. (2008). Solving the test-field equations allows us to calculate $\overline{\mathcal{E}}^{pq} = \overline{\boldsymbol{u} \times \boldsymbol{b}^{pq}}$ and, via equation (5), all 4+4 components of α_{ij} and η_{ij}.

Important control parameters are the magnetic Reynolds and Prandtl numbers, $\mathrm{Re}_M = u_{\mathrm{rms}}/(\eta k_f)$ and $\mathrm{Pr}_M = \nu/\eta$, where $u_{\mathrm{rms}} = \langle \boldsymbol{u}^2 \rangle^{1/2}$ is the actual (magnetically affected) rms velocity and angular brackets denote volume averages. The smallest possible wavenumber in a triply periodic domain of size $L \times L \times L$ is $k_1 = 2\pi/L$. In order to achieve large values of

Re_M, the value of k_f/k_1 should be small, but still large enough to allow for a clear separation of scales between the domain scale and the energy-carrying scale. We use $k_f/k_1 = 3$ as a compromise.

The structure of the turbulence is determined by the vectors $\overline{\boldsymbol{B}}$ and $\overline{\boldsymbol{J}}$, but for a Beltrami field they are aligned, so we have

$$\alpha_{ij}(\overline{\boldsymbol{B}}) = \alpha_1(\overline{\boldsymbol{B}})\delta_{ij} + \alpha_2(\overline{\boldsymbol{B}})\hat{B}_i\hat{B}_j,$$

(6)

$$\eta_{ij}(\overline{\boldsymbol{B}}) = \eta_1(\overline{\boldsymbol{B}})\delta_{ij} + \eta_2(\overline{\boldsymbol{B}})\hat{B}_i\hat{B}_j,$$

(7)

where $\hat{\boldsymbol{B}}$ means the unit vector in the direction of $\overline{\boldsymbol{B}}$. When inserting this into the general expression for the electromotive force given above this reduces to $\overline{\mathcal{E}} = \alpha\overline{\boldsymbol{B}} - \mu_0\eta_t\overline{\boldsymbol{J}}$, with coefficients

$$\alpha = \alpha_1 + \alpha_2 - \eta_2 k_m \quad \text{and} \quad \eta_t = \eta_1,$$

(8)

where $k_m = k_m(z, t) \equiv \mu_0\overline{\boldsymbol{J}} \cdot \overline{\boldsymbol{B}}/\overline{\boldsymbol{B}}^2$ is a pseudoscalar that quantifies the helicity of the large-scale field. (Here $k_m/k_1 \approx -1$.) We emphasize that for Beltrami fields the assignment of α_1, α_2, η_1, and η_2 to α and η_t is not unique. In the general situation, when the mean field is not of Beltrami type, instead of α_2 and η_2 eight new coefficients emerge which contribute in an unambiguous way to field generation and dissipation. Future work must show whether our α_1 and η_t are then still dominant.

3. RESULTS

Throughout this Letter we fix $\mathrm{Pr}_M = 1$ and vary Re_M between 2 and 600. For large values of Re_M a broader range of scales is excited, as can be seen in spectra of kinetic and magnetic energy, E_K and E_M, shown in Figure 1. In the range $4 < k/k_1 < 30$ both spectra are comparable to a $k^{-3/2}$ spectrum. For comparison, spectra of kinetic and magnetic helicity, H_K and H_M, are also shown.

For $\mathrm{Re}_M \leq 2$ there is no dynamo action, but in all other cases a large-scale magnetic field is maintained (Fig. 2), just as in Brandenburg (2001), except that here $k_f/k_1 = 3$ instead of 5 or larger. The dynamo is of α^2 type and hence the mean field a Beltrami field,

$$\overline{\boldsymbol{B}}(z, t) = \overline{B}(t)(\cos\theta, \sin\theta, 0), \quad \theta = k_1 z + \phi,$$

(9)

with phase ϕ. To shorten the transient phase we use this field also as initial condition.

Inserting equation (9) into equations (6) and (7) and calculating suitable averages over z (or volume) we get

$$\alpha_2 = 8\langle\alpha_{12}\cos\theta\sin\theta\rangle = 8\langle\alpha_{21}\cos\theta\sin\theta\rangle,$$

(10)

$$\alpha_1 + \alpha_2/2 = \langle\alpha_{11}\rangle = \langle\alpha_{22}\rangle,$$

(11)

and analogous for η_1 and η_2. Obviously, the determination of α_1, α_2, η_1, and η_2 requires knowledge of the Beltrami phase ϕ, which often drifts away from its initial value during the course of the run. We determine therefore the actual phase $\phi(t)$ by applying a suitable Fourier analysis to $\overline{\boldsymbol{B}}$.

In general, α-quenching can involve time derivatives (e.g., Kleeorin & Ruzmaikin 1982; BB02). In order to avoid such complications we focus on statistically steady (dynamo) solutions, that is, on the saturated dynamo fields. For given values
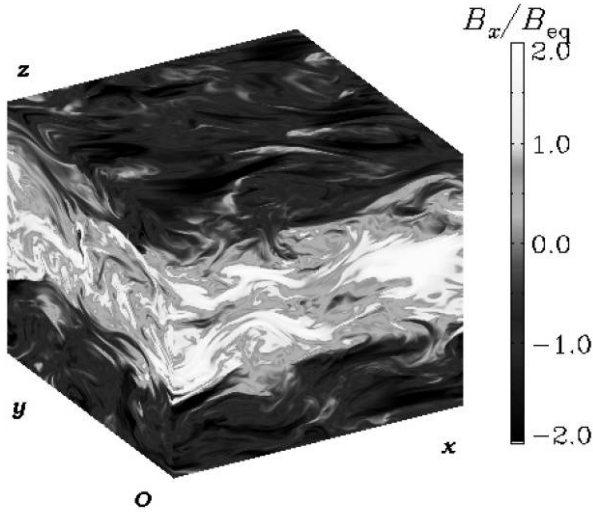
Fig. 2.—Visualization of B_x on the periphery of the computational domain for a run with $\mathrm{Re}_M = 600$ and a resolution of 512^3 mesh points. Note that on average the field is compatible with that in eq. (9). Note also the clear anisotropy with structures elongated in the direction of the field. For an animation see http://www.nordita.org/software/pencil-code/movies/icascade/.

of the parameters of the system (1)–(3), the saturation strength of $\overline{\boldsymbol{B}}$ is uniquely determined. Hence, by changing the forcing strength or η we are only able to follow a specific path in the $\overline{B}$-Re_M plane, but not to scan it in a 2D fashion.

In Table 1 we represent the results in nondimensional form with normalized quantities indicated by a tilde. We normalize the rms values of the mean field and the fluctuations with the equipartition field strength $B_{\mathrm{eq}}^2 = \mu_0 \langle \rho u^2(\overline{\boldsymbol{B}}) \rangle$ and introduce

$$\tilde{\eta}_1 = \eta_1/\eta_{t0}, \quad \tilde{\eta}_2 = \eta_2/\eta_{t0}, \quad \tilde{\eta} = \eta/\eta_{t0}, \quad (12)$$

$$\tilde{\alpha}_1 = \alpha_1/\alpha_0, \quad \tilde{\alpha}_2 = \alpha_2/\alpha_0, \quad (13)$$

where $\eta_{t0} = \frac{1}{3} u_{\mathrm{rms}}(\overline{\boldsymbol{B}}) k_f^{-1}$, $\alpha_0 = -\frac{1}{3} u_{\mathrm{rms}}(\overline{\boldsymbol{B}})$, and $u_{\mathrm{rms}}(\overline{\boldsymbol{B}})$ is the rms velocity of the saturated state, so the reference values are already magnetically affected. This normalization implies that in the kinematic case $\tilde{\alpha}_1 = \tilde{\eta}_1 = 1$ (Sur et al. 2008), while $\tilde{\alpha}_2 = \tilde{\eta}_2 = 0$. Error bars are calculated based on the maximum departure obtained from the three time series, each taken over one third of the full sequence.

The consistency of the results for α and η_t with the presence of a steady state can be assessed by calculating the growth rate, λ, of the associated kinematic mean field dynamo for a Beltrami field with $k_m = -k_1$, i.e., $\lambda = -\alpha k_1 - (\eta_t + \eta)k_1^2$. In the sat-

urated state λ should vanish. Again, we present λ in nondimensional form, here in terms of the turbulent decay rate,

$$\tilde{\lambda} \equiv \lambda/(\eta_{t0} k_1^2) = \tilde{\alpha} \tilde{k}_f - (\tilde{\eta}_t + \tilde{\eta}), \quad (14)$$

where $\tilde{\alpha} = \alpha/\alpha_0$ and $\tilde{k}_f = k_f/k_1$. Within error bars, the value of λ is consistent with zero, thus supporting the consistency of α and η_t with the established steady state; see Table 1. (An exception is Run A, because it is subcritical and so $\lambda < 0$.) This in turn supports the applicability of the test-field method to the nonlinear case. However, as in almost all supercritical runs a small-scale dynamo is operative, our results which are derived under the assumption of its influence being negligible may contain a systematic error. If present, it should be small, though, given the good precision of the results for λ. A more thorough study of the role of the small-scale dynamo will be the subject of future work.

A measure of the reliability of the averages is the length of the time series in "turnover" times, $\Delta \tilde{t} = u_{\mathrm{rms}} k_f (t_{\max} - t_{\min})$. Our results presented in Table 1 show a decline of $\tilde{\alpha}$ by a factor ≈ 15 and a decline of $\tilde{\eta}_t$ by a factor ≈ 5 as Re_M increases by a factor 300 while $\overline{B} = (0.9$–$1.4)B_{\mathrm{eq}}$.

As expected, there are random fluctuations of α and η_t, represented here by their non-dimensional rms values, $\tilde{\alpha}_{\mathrm{rms}} = \alpha_{\mathrm{rms}}/\alpha_0$ and $\tilde{\eta}_{\mathrm{rms}} = \eta_{\mathrm{rms}}/\eta_{t0}$. Even for large Re_M the fluctuations remain around 0.1 and 0.2, respectively. This is less than in the kinematic case (Brandenburg et al. 2008), but still comparable to the mean values of $\tilde{\alpha}$ and $\tilde{\eta}_t$, respectively.

4. DISCUSSION

Let us now put our results in relation to earlier work, which mostly used mean fields defined as full volume averages, hence being uniform. In that case α was quenched all the way to zero like Re_M^{-1}. This result can be understood in terms of a mutual cancellation of kinetic and magnetic contributions to the α effect (Pouquet et al. 1976),

$$\alpha = \alpha_K + \alpha_M, \quad \alpha_K = -\tfrac{1}{3} \tau \overline{\boldsymbol{\omega} \cdot \boldsymbol{u}}, \quad \alpha_M = \tfrac{1}{3} \tau \overline{\boldsymbol{j} \cdot \boldsymbol{b}} / \overline{\rho}, \quad (15)$$

where $\boldsymbol{\omega} = \nabla \times \boldsymbol{u}$. Assuming $\tau u_{\mathrm{rms}} k_f \approx 1$ (Brandenburg & Subramanian 2007), we estimate τ and hence, by measuring $\boldsymbol{\omega} \cdot \boldsymbol{u}$ and $\boldsymbol{j} \cdot \boldsymbol{b}$, we determine $\tilde{\alpha}_K = \alpha_K/\alpha_0$ and $\tilde{\alpha}_M = \alpha_M/\alpha_0$; see Table 1 and Figure 3. It turns out that $\tilde{\alpha}_K$ is essentially independent of Re_M and $\tilde{\alpha}_M$ approaches a certain fraction of $\tilde{\alpha}_K$, reducing the residual α in equation (15) as Re_M increases. This agrees only qualitatively with the measured decline of $\tilde{\alpha}$, because the residual α is still too big. However, equation (15) assumes isotropy and that the values of τ are the same for α_K and α_M, which is not borne out by simulations (Brandenburg & Subramanian 2007). By contrast, our direct calculation

TABLE 1
Transport Coefficients for Runs in the Range $2 \leq \mathrm{Re}_M \leq 600$ at Saturation Field Strengths

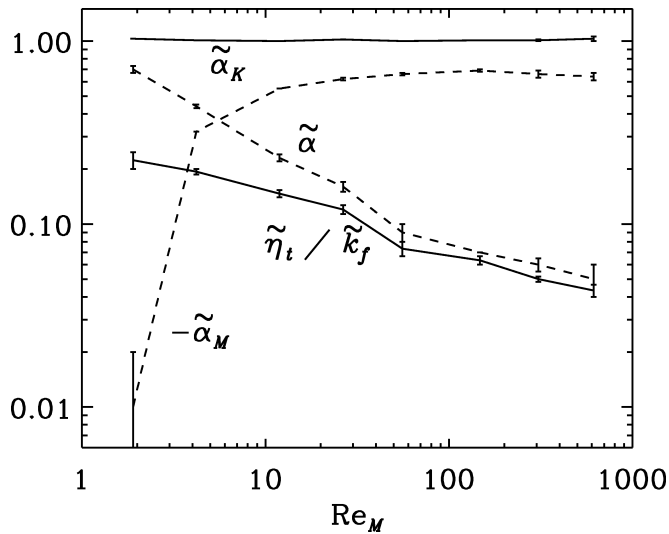| Run	Re_M	$\tilde{B}^2$	$\tilde{b}^2$	$\tilde{\alpha}$	$\tilde{\eta}_t$	$\tilde{\eta}$	$\tilde{\lambda}$	$-\tilde{\alpha}_2$	$-\tilde{\eta}_2$	$\tilde{\alpha}_{\mathrm{rms}}$	$\tilde{\eta}_{\mathrm{rms}}$	$+\tilde{\alpha}_K$	$-\tilde{\alpha}_M$	$\Delta\tilde{t}$
A	2	0.0	0.0	0.70 ± 0.03	0.67 ± 0.07	1.57	-0.14 ± 0.01	0.04 ± 0.05	-0.02 ± 0.06	0.09	0.12	1.03	0.01	150
B	4	0.9	0.4	0.44 ± 0.01	0.58 ± 0.02	0.72	0.01 ± 0.00	0.34 ± 0.02	-0.12 ± 0.01	0.11	0.22	1.01	0.32	736
C	12	1.7	0.7	0.23 ± 0.01	0.44 ± 0.02	0.25	-0.02 ± 0.01	0.39 ± 0.02	-0.04 ± 0.01	0.08	0.16	1.00	0.55	682
D	30	1.9	0.8	0.16 ± 0.01	0.36 ± 0.02	0.11	-0.00 ± 0.01	0.37 ± 0.04	0.03 ± 0.03	0.07	0.14	1.02	0.62	350
E	60	2.0	0.8	0.09 ± 0.01	0.22 ± 0.02	0.05	0.00 ± 0.01	0.33 ± 0.01	0.05 ± 0.01	0.09	0.22	1.00	0.66	711
F	150	2.0	0.9	0.07 ± 0.00	0.19 ± 0.01	0.02	0.01 ± 0.01	0.24 ± 0.05	0.08 ± 0.01	0.07	0.16	1.01	0.69	225
G	300	1.8	0.9	0.06 ± 0.00	0.15 ± 0.00	0.01	0.01 ± 0.01	0.21 ± 0.02	0.05 ± 0.02	0.06	0.16	1.01	0.66	177
H	600	1.8	0.9	0.05 ± 0.01	0.13 ± 0.01	0.005	0.01 ± 0.04	0.14 ± 0.05	0.04 ± 0.01	0.05	0.10	1.03	0.64	44

FIG. 3.—Re_M-dependence of $\tilde{\alpha}$ and $\tilde{\eta}_t/\tilde{k}_f$ together with $\tilde{\alpha}_K$ and $-\tilde{\alpha}_M$.

η_t. The consistency of the results of the test-field method suggest that the nonlinear α can be determined from the knowledge of $\boldsymbol{u}(\boldsymbol{x}, t)$ over several past correlation times. Qualitatively, the quenching of α can be explained by $-\alpha_M$ approaching α_K for finite field strengths and large Re_M. Generally, α will be quenched to whatever is the value of $(\eta_t + \eta)k_1$ (BB02). However, until now we had no idea how big the quenched value of η_t is. There was the possibility that η_t was quenched to very small values, just like in the two-dimensional case (Cattaneo & Vainshtein 1991). If that were true, α would also be very small. We can now say that this is not the case, because η_t is only reduced to about 20% of the kinematic value, while the normalized value $\tilde{\alpha}$ is quenched to $\approx \tilde{\eta}_t/\tilde{k}_f \approx 7\%$ of its kinematic value, as is seen in Figure 3.

Obvious extensions of this work include the application to non-Beltrami fields and to domains with boundaries and/or shear. In the latter case there exists a great deal of earlier work with relevant simulation data supporting the idea of an α effect that is strongly controlled by magnetic helicity evolution, and that catastrophic quenching can be decisively alleviated in the presence of shear-driven magnetic helicity fluxes.

shows that $\tilde{\alpha}$ is quenched to values of order $\tilde{\eta}_t/\tilde{k}_f$, as is necessary for a steady state; see equation (14). Note that the decline of $\tilde{\eta}_t$ is much weaker than in the two-dimensional case where η_t decreases like Re_M^{-1} (Cattaneo & Vainshtein 1991).

5. CONCLUSIONS

For the first time it has been possible to determine both α_{ij} and η_{ij} in the magnetically quenched case. These tensors are here characterized by the non-tensorial quantities α and

REFERENCES

Blackman, E. G., & Brandenburg, A. 2002, ApJ, 579, 359 (BB02)
Brandenburg, A. 2001, ApJ, 550, 824
Brandenburg, A., & Subramanian, K. 2007, Astron. Nachr., 328, 507
Brandenburg, A., et al. 2008, ApJ, 676, 740
Cattaneo, F., & Hughes, D. W. 1996, Phys. Rev. E, 54, R4532
Cattaneo, F., & Vainshtein, S. I. 1991, ApJ, 376, L21

Kleeorin, N., & Rogachevskii, I. 1999, Phys. Rev. E, 59, 6724
Kleeorin, N. I., & Ruzmaikin, A. A. 1982, Magnetohydrodynamics, 18, 116
Pouquet, A., Frisch, U., & Léorat, J. 1976, J. Fluid Mech., 77, 321
Sur, S., Brandenburg, A., & Subramanian, K. 2008, MNRAS, 385, L15
Vainshtein, S. I., & Cattaneo, F. 1992, ApJ, 393, 165
Yousef, T. A., Brandenburg, A., & Rüdiger, G. 2003, A&A, 411, 321